

December, 1999
OU-HEP-338
hep-ph/9912500

Spin and Orbital Angular Momentum Distribution Functions of the Nucleon

M. Wakamatsu¹

Department of Physics, Faculty of Science,
Osaka University,
Toyonaka, Osaka 560, JAPAN

T. Watabe²

Research Center for Nuclear Physics (RCNP),
Osaka University,
Ibaraki, Osaka 567, JAPAN

PACS numbers : 12.39.Fe, 12.39.Ki, 12.38.Lg, 13.60.-r

Keywords : Chiral quark model, Orbital angular momentum, Evolution

Abstract

A theoretical prediction is given for the spin and orbital angular momentum distribution functions of the nucleon within the framework of an effective quark model of QCD, i.e. the chiral quark soliton model. An outstanding feature of the model is that it predicts fairly small quark spin fraction of the nucleon $\Delta\Sigma \simeq 0.35$, which in turn dictates that the remaining 65 % of the nucleon spin is carried by the orbital angular momentum of quarks and antiquarks at the model energy scale of $Q^2 \simeq 0.3 \text{ GeV}^2$. This large orbital angular momentum necessarily affects the scenario of scale dependence of the nucleon spin contents in a drastic way.

¹Email : wakamatu@miho.rcnp.osaka-u.ac.jp

²Email : watabe@rcnp.osaka-u.ac.jp

1 Introduction

The recent renewal of interest in polarized lepton-hadron and hadron-hadron deep-inelastic scatterings greatly owes to the so-called “nucleon spin crisis” aroused by the EMC experiment [1]. According to the latest SMC analysis [2], the intrinsic quark spin carries only about 20 % of the total nucleon spin. The widely-believed resolution of this puzzle is based on an assumption of large gluon polarization [3]. In fact, the recent next-to-leading-order (NLO) analyses of the polarized deep-inelastic-scattering (DIS) data for $g_1(x, Q^2)$ appear to indicate a positive value for the gluon polarization [4]. Nevertheless, the situation is far from conclusive, since the result of these analyses is rather sensitive to the input shapes of the polarized distributions as well as the uncertainties of the available polarized DIS data.

Although somewhat nonstandard, there is another scenario that also leads to qualitative resolution of the nucleon spin problem. This scenario was first introduced on the basis of the Skyrme model [5]. Later, the idea was developed into a more quantitative one within the framework of the chiral quark soliton model (CQSM) [6],[7]. The CQSM is an effective quark model of QCD, which was first introduced by Diakonov and Petrov, based on the instanton-liquid picture of the QCD vacuum [8],[9]. Being in conformity with Witten’s idea of large N_c QCD [11], it shares many features in common with the Skyrme model [12],[13] at least in the ideal limit of $N_c = \infty$. (For review, see [10].) At the subleading order of $1/N_c$ expansion, however, several crucial differences have been found to exist between them [7],[14],[15]. Among others, most important would be the following two. The first is the $1/N_c$ correction (or the first order rotational correction in the collective angular velocity Ω) to the isovector axial-vector coupling constant of the nucleon, which definitely exists in the CQSM but is entirely missing in the Skyrme model [15]. (In our opinion, this solves the so-called “ g_A problem” in the latter [14].) The second concerns the subject of our central interest here, i.e. the predictions for the quark spin fraction $\Delta\Sigma$ of the nucleon. As was first noticed by Brodsky et al. [5], $\Delta\Sigma$ identically vanishes in the naive Skyrme model. At first sight, this appeared to be a favorable feature of the model since it looks consistent with the result of the EMC measurement [1]. As we have argued repeatedly [7],[14], however, this outstanding prediction of the Skyrme model should be taken with care, because it just arises from the fact that this model cannot correctly describe the physics at the subleading order of $1/N_c$ expansion. In fact, the presence of the next-to-leading order contribution to $\Delta\Sigma$ is again a distinguishable feature of the CQSM as compared with the naive Skyrme model [7]. Nonetheless, qualitative similarity between the two models still survives and the prediction of the CQSM for $\Delta\Sigma$ remains to be fairly small, i.e. $\Delta\Sigma \simeq 0.35$, as compared with other effective models of the nucleon like the nonrelativistic

quark model or the MIT bag model. What carries the rest of the nucleon spin ? Within the CQSM, the answer to this question is quite simple. It must be the orbital angular momentum of quarks and/or antiquarks, since it is an effective theory with the effective quark degrees of freedom only [7].

A natural question is whether the effective quark degrees of freedom are enough to describe the relevant physics. One might suspect that the gluon polarization or its orbital angular momentum may play important roles even at the low energy hadronic scale. There have been some attempts to introduce the explicit gluon degrees of freedom into the CQSM in reference to the underlying instanton-liquid picture of the QCD vacuum [17],[18]. Unfortunately, the situation is far from conclusive yet. Here we simply assumes that the explicit gluonic degrees of freedom are not crucial at least for the polarized distribution functions at the low renormalization point, which is taken to be the starting energy of the DGLAP evolution equation. That this is not a meaningless assumption can, for instance, be convinced from our recent analysis of the longitudinally polarized distribution functions of the nucleon and the deuteron in comparison with the recent EMC and SMC data [19],[20]. This analysis starts with the predictions of the CQSM for the longitudinally polarized distribution functions for quarks and antiquarks, which are taken to be input distributions given at the model energy scale of $Q_{ini}^2 = 0.3 \text{ GeV}^2$. The polarized distribution functions for the gluon are simply assumed to be zero at this initial energy scale. After solving the standard evolution equation at the NLO, the predictions of the model were then compared with the recent EMC and SMC data for $g_1^p(x, Q^2)$, $g_1^n(x, Q^2)$, and $g_1^d(x, Q^2)$ given at $Q^2 = 5 \text{ GeV}^2$ [2]. Despite the rather drastic assumption of zero gluon polarization at the hadronic scale, the theory was shown to reproduce all the qualitatively noticeable features of the experimental data.

Encouraged by this success, now we push forward our attempts to clarify the spin contents of the nucleon. That is, the main purpose of the present study is to give a theoretical prediction for the orbital angular momentum distribution functions for quarks and antiquarks in the nucleon. After combining those with the previously-obtained quark spin distribution functions, we can investigate the scale dependence of the full nucleon spin contents by using the recently-derived evolution equation at the leading order (LO) [22],[23]. (We however recall fact that there is a criticism against this LO evolution equation for the orbital angular momentum distributions [24].) Although our analysis is bound to one basic assumption that the gluon polarization as well as the gluon orbital angular momentum play no significant role at least at the hadronic scale of $Q^2 \leq 0.3 \text{ GeV}^2$, it is expected to provide us with quite a unique scenario for the scale dependence of the nucleon spin content, while keeping satisfactory agreement with the available high-energy data for $g_1^p(x, Q^2)$, $g_1^n(x, Q^2)$, and $g_1^d(x, Q^2)$.

We shall explain in the next section the theoretical framework which our calculation of the orbital angular momentum distribution functions for quarks and antiquarks are based on. Next, we discuss the scale dependence of the nucleon spin contents including the orbital angular momentum based on the given input distributions at the low renormalization point. Finally, we summarize our findings in the last section.

2 The theoretical framework

How to treat the orbital angular momentum has been one of the most controversial theoretical problems in hadron spin physics. It is well known that the most natural definition of angular momentum is not gauge invariant [25]. Recently, Bashinsky and Jaffe proposed a gauge-invariant formulation of the angular momentum for quarks and gluons which reduces to natural definition in a particular gauge, i.e. the light-cone gauge $A^+(x) = 0$ [26]. It was also suggested [27] that this gauge invariant formulation may give an extended support to the recently derived LO evolution equation for the orbital angular momentum distributions in the light-cone gauge [22],[23]. According to the authors of [24], however, nonlocal operators with dependence on spatial coordinates have not been seen in factorization of hard forward scattering processes, and in particular inclusive deep-inelastic scatterings do not depend on such types of operators. Accordingly, the evolution of the orbital angular momentum distributions would become extremely complicated in the light-cone gauge contrary to the results of [22],[23]. On the other hand, there is another definition of orbital angular momentum distributions, which maintains gauge invariance at the cost of losing full Lorentz covariance [24]. This latter definition has its meaning only in a limited class of coordinates in which the nucleon has a definite helicity. An advantage of the second definition is that it can be extracted from the polarized and unpolarized quark distributions and the off-forward distributions $E(x)$ so that it can in principle be measured. What is not fully clarified yet is the relation between these two definitions of angular momentum distributions. In sum, the proper definition of the orbital angular momentum distributions as well as the corresponding evolution equation in QCD is still an unsettled issue being subject to a debate. One should therefore take the following investigation of the orbital angular momentum distribution within an effective theory of QCD bearing all these affairs in mind.

Since the CQSM at the present level of approximation contains no gluonic degrees of freedom at least explicitly, it seems natural to start with the following naive definition of the

quark orbital angular momentum distribution function :

$$q_L(x) = \frac{1}{\sqrt{2}p^+} \int_{-\infty}^{\infty} \frac{d\lambda}{2\pi} e^{i\lambda x} \langle PS_3 | \psi_+^\dagger(0) i (x^1 \partial^2 - x^2 \partial^1) \psi_+(\lambda n) | PS_3 \rangle, \quad (1)$$

Here p^μ and n^μ are two light-like (null) vectors, having the properties

$$p^- = 0, \quad n^+ = 0, \quad p^2 = n^2 = 0, \quad p \cdot n = 1, \quad (2)$$

while ψ_+ is a component of the quark field ψ defined through the decomposition

$$\psi = (P_+ + P_-) \psi = \psi_+ + \psi_-, \quad (3)$$

by the projection operators $P_\pm = \frac{1}{2} \gamma^\mp \gamma^\pm$ with $\gamma^\pm = (1/\sqrt{2})(\gamma^0 \pm \gamma^3)$. Extending the definition of distribution function $q_L(x)$ to interval $-1 \leq x \leq 1$, the relevant antiquark distributions are given as

$$\bar{q}_L(x) = q_L(-x), \quad (0 < x < 1). \quad (4)$$

Naturally, from more general viewpoint of underlying color gauge theory, i.e. QCD, the naive definition (1) is not gauge invariant and holds only in the light-cone gauge. As was already explained, this definition of the quark orbital angular momentum is not free from problems, especially when we are to use it as a initial distribution of scale evolution. We expect that this is not so serious for our investigation below, since our main concern there is the qualitative behavior of the quark orbital angular momentum distribution at the model scale, which naturally has a strong correlation with the quark spin distribution at the same scale. On the other hand, the study of its scale dependence should be taken as semi-qualitative one.

The basis of our theoretical analysis is the following path integral representation of the nucleon matrix element of bilocal quark operator [28] :

$$\begin{aligned} \langle N(\mathbf{P}) | \psi^\dagger(0) O \psi(z) | N(\mathbf{P}) \rangle &= \frac{1}{Z} \int d^3x d^3y e^{-i\mathbf{P}\cdot\mathbf{x}} e^{i\mathbf{P}\cdot\mathbf{y}} \int \mathcal{D}\pi \int \mathcal{D}\psi \mathcal{D}\psi^\dagger \\ &\times J_N\left(\frac{T}{2}, \mathbf{x}\right) \cdot \psi^\dagger(0) O \psi(z) \cdot J_N^\dagger\left(-\frac{T}{2}, \mathbf{y}\right) e^{i \int d^3x \mathcal{L}_{CQM}}, \end{aligned} \quad (5)$$

where

$$\mathcal{L}_{CQM} = \bar{\psi} (i \not{\partial} - M e^{i\gamma_5 \boldsymbol{\tau} \cdot \boldsymbol{\pi}(x)/f_\pi}) \psi, \quad (6)$$

is the basic lagrangian of the CQSM, while

$$J_N(x) = \frac{1}{N_c!} \epsilon^{\alpha_1, \dots, \alpha_{N_c}} \Gamma_{JJ_3, TT_3}^{f_1, \dots, f_{N_c}} \psi_{\alpha_1 f_1}(x) \cdots \psi_{\alpha_{N_c} f_{N_c}}(x), \quad (7)$$

is a composite operator carrying the quantum numbers JJ_3, TT_3 (spin, isospin) of the nucleon, where α_i is the color index, while $\Gamma_{JJ_3, TT_3}^{f_1, \dots, f_{N_c}}$ is a symmetric matrix in spin-flavor indices f_i . We start with a stationary pion field configuration of hedgehog shape :

$$\boldsymbol{\pi}(x) = f_\pi \hat{\mathbf{r}} F(r). \quad (8)$$

Next we carry out a path integral over $\boldsymbol{\pi}(x)$ in a saddle point approximation by taking care of two zero-energy modes, i.e. the translational zero-modes and rotational zero-modes. Under the assumption of ‘‘slow rotation’’ as compared with the intrinsic quark motion, the answer can be obtained in a perturbative series in Ω , which can also be regarded as a $1/N_c$ expansion. The first nonvanishing contribution to $q_L(x)$ arises at the $O(\Omega^1)$ term of this expansion, since the leading $O(\Omega^0)$ term vanishes identically due to the hedgehog symmetry. According to the general formalism derived in [19], the answer is given in the following form :

$$\Delta q_L(x) = \Delta q_L^{\{A,B\}}(x) + \Delta q_L^C(x), \quad (9)$$

where

$$\begin{aligned} \Delta q_L^{\{A,B\}} &= \langle J_3 \rangle_{p\uparrow} \cdot M_N \frac{N_c}{I} \sum_{m=\text{all}, n \leq 0} \frac{1}{E_m - E_n} \langle n | \tau_3 | m \rangle \langle m | (1 + \gamma^0 \gamma^3) L_3 \delta_n | n \rangle \\ &= - \langle J_3 \rangle_{p\uparrow} \cdot M_N \frac{N_c}{I} \sum_{m=\text{all}, n > 0} \frac{1}{E_m - E_n} \langle n | \tau_3 | m \rangle \langle m | (1 + \gamma^0 \gamma^3) L_3 \delta_n | n \rangle, \end{aligned} \quad (10)$$

and

$$\begin{aligned} \Delta q_L^C(x) &= \langle J_3 \rangle_{p\uparrow} \cdot \frac{d}{dx} \frac{N_c}{2I} \sum_{n \leq 0} \langle n | \tau_3 (1 + \gamma^0 \gamma^3) L_3 \delta_n | n \rangle \\ &= - \langle J_3 \rangle_{p\uparrow} \cdot \frac{d}{dx} \frac{N_c}{2I} \sum_{n > 0} \langle n | \tau_3 (1 + \gamma^0 \gamma^3) L_3 \delta_n | n \rangle, \end{aligned} \quad (11)$$

with $L_3 \equiv -i(x^1 \partial^2 - x^2 \partial^1)$ and $\delta_n \equiv \delta(xM_N - E_n - p_3)$, while $\langle \mathcal{O} \rangle_{p\uparrow}$ denotes a matrix element of a collective space operator \mathcal{O} with respect to the proton in the spin up state along the z -axis, i.e.

$$\langle \mathcal{O} \rangle_{p\uparrow} = \int \Psi_{(1/2)(1/2)}^{(1/2)}[\xi_A] \mathcal{O} \Psi_{(1/2)(1/2)}^{(1/2)}[\xi_A] d\xi_A = \langle p, S_3 = 1/2 | \mathcal{O} | p, S_3 = 1/2 \rangle. \quad (12)$$

Here, $|m\rangle$ and E_m are the eigenstates and the associated eigenenergies of the static hamiltonian $H = -i\boldsymbol{\alpha} \cdot \boldsymbol{\nabla} + \beta M e^{i\gamma_5 \boldsymbol{\tau} \cdot \hat{\mathbf{r}} F(r)}$ with the hedgehog background. Note that both of $\Delta q_L^{\{A,B\}}(x)$ and $q_L^C(x)$ are represented in two equivalent forms, i.e. in the occupied form ($n \leq 0$) convenient for the numerical calculation for $x > 0$ and in the nonoccupied form ($n > 0$) convenient for $x < 0$.

In the actual numerical calculation, the expression of any physical quantity is divided into two pieces, i.e. the contribution of what we call the valence quark level (it is the lowest energy eigenstate of the static hamiltonian H , which emerges from the positive energy continuum) and that of the Dirac sea quarks (the latter is also called the vacuum polarization contribution) as explained in [19]. Since the latter contains ultraviolet divergences, it must be regularized. Here we use the so-called Pauli-Villars regularization scheme [28]. The regulator mass M_{PV} of this cutoff scheme is determined uniquely from the physical requirement that the effective meson action derived from (6) gives correct normalization for the pion kinetic term. Using the value of $M = 375$ MeV, which is favored from the phenomenology of nucleon low energy observables, this condition gives $M_{PV} \simeq 562$ MeV. Since we are to use these values of M and M_{PV} , there is *no free parameter* additionally introduced in the calculation of distribution functions.

3 Numerical Results and Discussion

We first show in Fig.1 the theoretical predictions for the orbital angular momentum distribution functions of quarks and antiquarks as well as the isosinglet quark polarization. (The latter was already given in [19], but it is shown here again for emphasizing how the x -dependences of the two distributions are different.) Here the distribution with negative x are to be interpreted as the antiquark distribution according to the rule (4) and the similar relation for $\Delta\bar{u}(x) + \Delta\bar{d}(x)$. The long-dashed and dash-dotted curves respectively stand for the contribution of the discrete valence level and that of the negative energy Dirac sea, while their sum is shown by the solid curves. As already noticed in [19], the contribution of Dirac sea is not so significant for $\Delta u(x) + \Delta d(x)$. The situation is quite different for the orbital angular momentum distribution $q_L(x)$. One clearly sees that the contribution of the polarized Dirac vacuum being peaked around $x \simeq 0$ is dominating over that of the discrete valence level. This can also be convinced from the first moment defined by

$$L_q = \int_{-1}^1 q_L(x) dx = \int_0^1 [q_L(x) + \bar{q}_L(x)] dx. \quad (13)$$

The contributions of the Dirac continuum and of the discrete valence level to this moment are respectively 0.195 and 0.130, which shows that the former dominates over the latter. The sum of these two numbers gives $L_q \simeq 0.325$, which means that about 65 % of the nucleon spin is

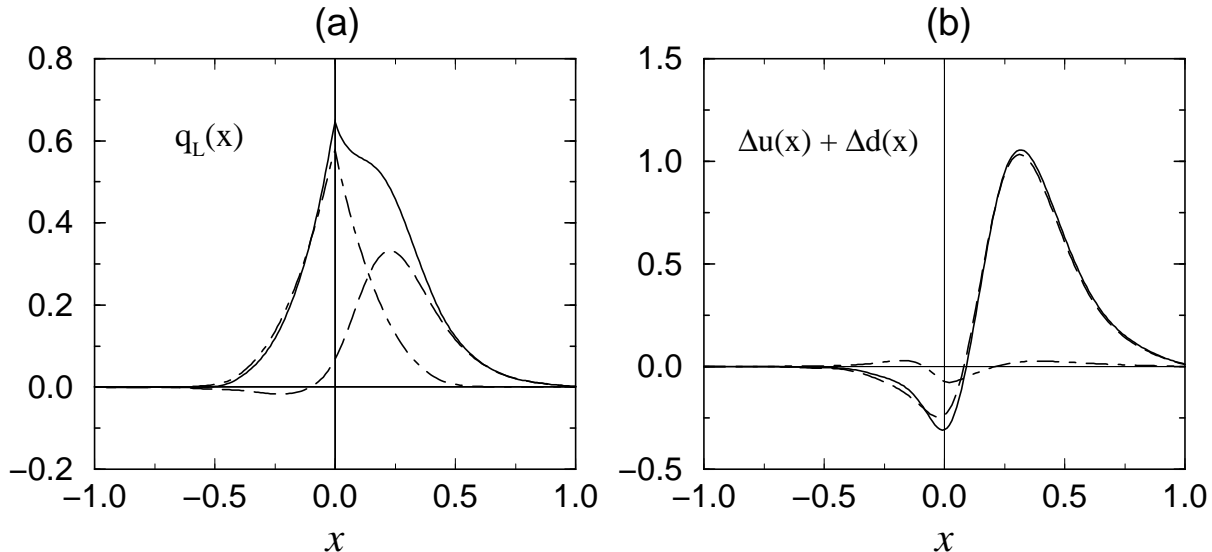


Figure 1: (a) The theoretical predictions of the CQSM for the quark and antiquark orbital angular momentum distribution functions $q_L(x)$ and (b) the isosinglet quark polarization $\Delta u(x) + \Delta d(x)$. The long-dashed and dash-dotted curves respectively stand for the contributions of the discrete valence level and that of the Dirac continuum in the self-consistent hedgehog background, whereas their sums are shown by the solid curves. The distributions with negative x are to be interpreted as the antiquark distributions.

carried by the orbital angular momentum of quarks and antiquarks at the energy scale of the model [7],[19].

We can also know the separate contributions of quarks and antiquarks to the total orbital angular momentum. They are shown in table 1 together with the corresponding separation for the quark spin fraction of the nucleon, or the flavor-singlet quark polarization $\Delta\Sigma$. One sees that the flavor-singlet polarization of antiquark is negative but fairly small in magnitude. (Note however that this does not necessarily mean that the polarizations of all the antiquarks are small. It has been shown [20] that the CQSM predicts fairly large isospin asymmetry of the longitudinally polarized antiquark distribution in the nucleon, i.e. $\Delta\bar{d}(x) - \Delta\bar{u}(x) < 0$.) On the contrary, a sizable amount ($\sim 30\%$) of the total orbital angular momentum is seen to be carried by antiquarks with soft (small x) component.

At this point, we want to make a short comment on the recent lattice QCD calculation of quark orbital angular momentum [29]. Aside from the fact that it is based on the so-called quenched approximation, one should also notice the fact that this is an indirect calculation of the quark orbital angular momentum L_q as well as the total gluon angular momentum J_g . They first extract the total quark angular momentum J_q from the calculation of the quark

Table 1: The separate contributions of quarks and antiquarks to the first moment $\Delta\Sigma$ and L_q at the scale of the model.

| | quark | antiquark | total |
|---------------------------------|-------|-----------|-------|
| $\Delta\Sigma$ | 0.397 | - 0.047 | 0.350 |
| L_q | 0.229 | 0.096 | 0.325 |
| $\frac{1}{2}\Delta\Sigma + L_q$ | 0.427 | 0.073 | 0.500 |

energy-momentum tensor form factors. Further combining the previous lattice calculation [30] of the quark spin content $\Delta\Sigma$, they obtain L_q , thereby extracting J_g from the total nucleon spin sum rule. This dictates that the extracted values of L_q and J_g would be sensitive to the uncertainties of J_q and $\Delta\Sigma$ obtained in the numerical simulation. The main conclusion of this analysis is that about 25% of the nucleon spin originates from the quark intrinsic spin, while about 35% comes from the quark orbital angular momentum, which in turn means that the remaining 40% of the nucleon spin is due to the glue. If this is confirmed by more precise calculation in the future, the present investigation done with neglect of the explicit gluonic degrees of freedom needs a considerable amendment. At least, some of the quark contributions obtained within the QCSM must be redistributed to either or both of the gluon spin and orbital angular momentum. It is interesting to see that scaling the CQSM predictions $\langle\frac{1}{2}\Delta\Sigma\rangle \simeq 35\%$ and $\langle L_q\rangle \simeq 65\%$ by the factor of 0.6, we would obtain $\langle\frac{1}{2}\Delta\Sigma\rangle \simeq 21\%$ and $\langle L_q\rangle \simeq 39\%$, which is rather close to the corresponding numbers 25% and 35% obtained in the above lattice QCD study. An interesting common feature in both theories is the dominance of the quark orbital angular momentum over the intrinsic quark spin fraction.

Now we are in a position to investigate the scale dependence of the full nucleon spin contents together with the corresponding distribution functions. As already mentioned, we assume that the gluon polarization and the gluon orbital angular momentum are both zero at the starting energy scale of $Q^2 = Q_{ini}^2$, i.e.

$$\Delta\Sigma(Q_{ini}^2) = 0.350, \quad \Delta g(Q_{ini}^2) = 0, \quad L_q(Q_{ini}^2) = 0.325, \quad L_g(Q_{ini}^2) = 0, \quad (14)$$

with the normalization

$$\frac{1}{2}\Delta\Sigma(Q^2) + \Delta g(Q^2) + L_q(Q^2) + L_g(Q^2) = \frac{1}{2}. \quad (15)$$

The question here is how to choose Q_{ini}^2 . In our previous analysis of the longitudinally polarized structure functions $g_1^p(x, Q^2)$, $g_1^n(x, Q^2)$ and $g_1^d(x, Q^2)$ based on the evolution equation at the

next-to-leading-order (NLO), a good agreement with the available high-energy data has been obtained with the choice $Q_{ini}^2 = 0.30 \text{ GeV}^2$ [19],[20]. Unfortunately, the evolution equation including the orbital angular momentum distributions is known only at the leading order (LO) [31]. Expecting that the use of a little smaller value of Q_{ini}^2 would compensate the defect of using this lower-order evolution equation, we proceed as follows. That is, we first solve the evolution equation for $\Delta\Sigma(Q^2)$ and $\Delta g(Q^2)$ at the NLO (in the \overline{MS} scheme) by setting $Q_{ini}^2 = 0.30 \text{ GeV}^2$ [32],[33]. Next, we solve the evolution equation for the full nucleon spin contents at the LO with use of a little smaller Q_{ini}^2 , i.e. $Q_{ini}^2 = 0.23 \text{ GeV}^2$, which is determined so as to roughly reproduce the Q^2 -evolution of the gluon polarization $\Delta g(Q^2)$ obtained by solving the NLO evolution with $Q_{ini}^2 = 0.30 \text{ GeV}^2$.

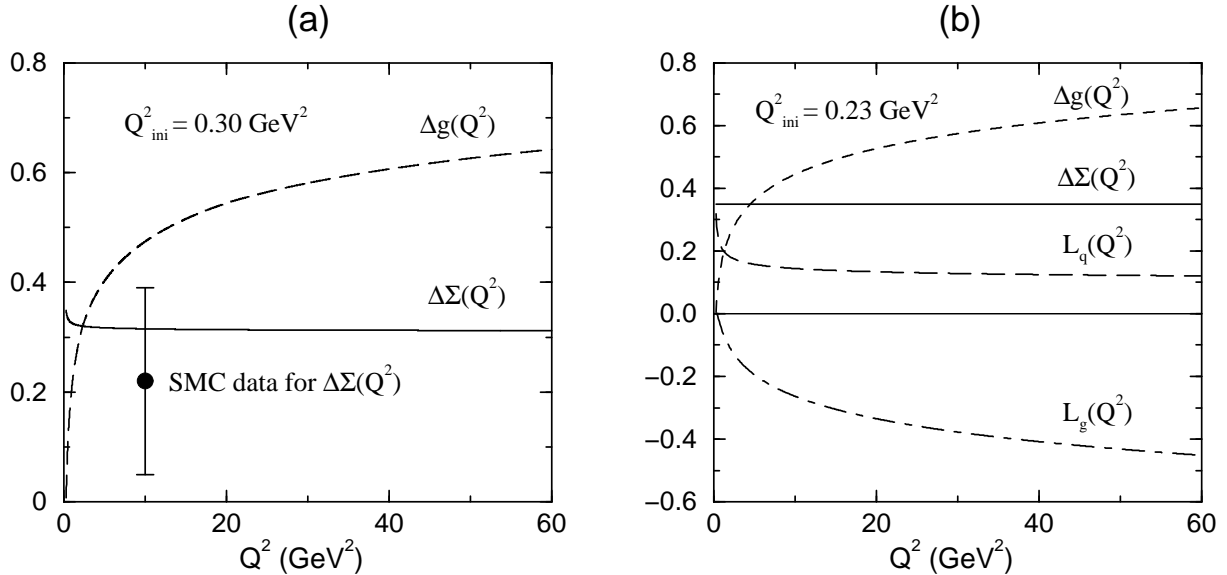


Figure 2: (a) The NLO evolutions of the flavor-singlet quark and gluon polarizations. The experimental data given at $Q^2 = 10 \text{ GeV}^2$ corresponds to the NLO analysis by the SMC group [2]. (b) The LO evolution of the full nucleon spin contents.

We first show in Fig.2(a) the NLO evolution for the quark and gluon polarization in comparison with the latest SMC data for $\Delta\Sigma(Q^2)$. One can say that the prediction of the CQSM for $\Delta\Sigma$ is qualitatively consistent with the recent NLO analysis of the SMC group given at $Q^2 = 10 \text{ GeV}^2$ [2]. One also sees that the gluon polarization rapidly grows with increasing Q^2 , even if we have assumed $\Delta g = 0$ at the initial energy scale of $Q_{ini}^2 = 0.30 \text{ GeV}^2$.

Shown in Fig.2(b) is the LO evolution of the full nucleon spin contents including the orbital angular momentum. They are calculated by using the known analytical solutions [31] :

$$\Delta\Sigma(Q^2) = \Delta\Sigma(Q_{ini}^2) = \text{constant}, \quad (16)$$

$$\Delta g(Q^2) = -\frac{12}{33-2n_f} \Delta \Sigma(Q_{ini}^2) + \frac{t}{t_0} \left(\Delta g(Q_{ini}^2) + \frac{12}{33-2n_f} \Delta \Sigma(Q_{ini}^2) \right), \quad (17)$$

$$L_q(Q^2) = -\frac{1}{2} \Delta \Sigma(Q_{ini}^2) + \frac{1}{2} \frac{3n_f}{16+3n_f} + \left(\frac{t}{t_0} \right)^{-\frac{2(16+3n_f)}{3(33-2n_f)}} \left(L_q(Q_{ini}^2) + \frac{1}{2} \Delta \Sigma(Q_{ini}^2) - \frac{1}{2} \frac{3n_f}{16+3n_f} \right), \quad (18)$$

$$L_g(Q^2) = -\Delta g(Q_{ini}^2) + \frac{1}{2} \frac{16}{16+3n_f} + \left(\frac{t}{t_0} \right)^{-\frac{2(16+3n_f)}{3(33-2n_f)}} \left(L_g(Q_{ini}^2) + \Delta g(Q_{ini}^2) - \frac{1}{2} \frac{16}{16+3n_f} \right), \quad (19)$$

with $t \equiv \ln Q^2 / \Lambda_{QCD}^2$, $t_0 \equiv \ln Q_{ini}^2 / \Lambda_{QCD}^2$ and $n_f = 3$. The starting energy of this evolution is taken to be $Q_{ini}^2 = 0.23 \text{ GeV}^2$, as mentioned above. As is widely-known, the flavor-singlet quark polarization $\Delta \Sigma$ is scale independent at the LO. Also relatively established is that the gluon polarization $\Delta g(Q^2)$ shows a logarithmic growth with increasing Q^2 , while it is largely compensated by the similar decrease of the gluon orbital angular momentum $L_q(Q^2)$. In fact, it was pointed out by Ji et al. [31] that, as $Q^2 \rightarrow \infty$, the sum of these two moments approaches its asymptotic value given by

$$J_q \equiv \Delta g + L_g \longrightarrow \frac{1}{2} \frac{16}{16+3n_f}, \quad (20)$$

which indicates (with $n_f = 3$) that about 64% of the nucleon spin is carried by the gluon fields in the asymptotic energy.

On the other hand, the evolution of quark orbital angular momentum is strongly dependent on the initial condition given at the low renormalization point. Since the scale-dependent factor

$$\left(\frac{t}{t_0} \right)^{-\frac{2(16+3n_f)}{3(33-2n_f)}}, \quad (21)$$

is a decreasing function of Q^2 (for $33 - 2n_f > 0$), we conclude that $L_q(Q^2)$ is a decreasing function of Q^2 as far as

$$L_q(Q_{ini}^2) + \frac{1}{2} \Delta \Sigma(Q_{ini}^2) - \frac{1}{2} \frac{3n_f}{16+3n_f}, \quad (22)$$

is positive, while it is an increasing function of Q^2 if the same quantity above is negative. In the case of the CQSM, it gives $L_q(Q_{ini}^2) + \frac{1}{2} \Delta \Sigma(Q_{ini}^2) - \frac{1}{2} \frac{3n_f}{16+3n_f} = 0.325 + 0.175 - 0.18 > 0$ at $Q^2 = Q_{ini}^2$, so that it is consistent with the fact that $L_q(Q^2)$ shown in Fig.3 is a decreasing function of Q^2 . The Q^2 dependence of $L_q(Q^2)$ looks strong only in the relatively lower Q^2 region, and beyond $Q^2 \simeq 5 \text{ GeV}^2$ it slowly approaches its asymptotic value given by

$$L_q(Q^2) \longrightarrow -\frac{1}{2} \Delta \Sigma(Q_{ini}^2) + \frac{1}{2} \frac{3n_f}{16+3n_f}. \quad (23)$$

Substituting our model predictions $\Delta\Sigma(Q_{ini}^2) = 0.35$ with $n_f = 3$, this gives $L_q \rightarrow 0.005$, which denotes that the quarks barely carry orbital angular momentum at the very high energy scale. Note, however, that the precise fraction of the quark orbital angular momentum in the asymptotic domain depends on the delicate cancellation of the two terms in (23).

It appears that the observation above contradicts one of the conclusions drawn in the recent paper by Scopetta and Vento [34]. They concluded that the quark orbital angular momentum can be important at large Q^2 , due to evolution, if it is not negligible at the scale of the hadronic model. It seems that this conclusion is mainly drawn from Fig.5(b) in [34], which shows that $L_q(Q^2)$ is an increasing function of Q^2 . This increasing behavior of $L_q(Q^2)$ appears to be inconsistent with the Q^2 -dependence of the quark orbital angular momentum distributions illustrated in Fig.4(a) of the same paper. In fact, the initial conditions of their ‘‘D-model’’ are given by $\Delta\Sigma(Q_{ini}^2) \simeq 0.4$, $\Delta g(Q_{ini}^2) \simeq 0.1$, $L_q(Q_{ini}^2) \simeq 0.145$, and $L_g(Q_{ini}^2) \simeq 0.055$. Since this gives $L_q(Q_{ini}^2) + \frac{1}{2} \Delta\Sigma(Q_{ini}^2) - \frac{1}{2} \frac{3n_f}{16+3n_f} = 0.165 > 0$, $L_q(Q^2)$ must be a decreasing function of Q^2 if our argument above is correct. Probably, the cause of discrepancy resides in an error in eqs.(17), (18) of [34]. The Q^2 -dependent factor $b^{-38/81}$ (with the definition $b = \alpha_S(Q^2)/\alpha_S(Q_{ini}^2)$) in (17) and (18) should be replaced by $b^{+50/81}$ for $n_f = 3$. (Note that $b^{-38/81}$ is an increasing function of Q^2 , while $b^{+50/81}$ is a decreasing function.)

Next, we show in Fig.3 the theoretical prediction of the CQSM for the spin and orbital angular momentum distribution functions and their LO evolutions. Here, we have used the LO evolution code provided by Martin et al. [27]. Here, the solid and long-dashed curves respectively represent $x \Delta\Sigma(x, Q^2)$ and $x L_q(x, Q^2)$, whereas the dashed and dash-dotted curves stand for $x \Delta g(x, Q^2)$ and $x L_g(x, Q^2)$. At the initial energy scale of $Q_{ini}^2 = 0.23 \text{ GeV}$, we set $\Delta g(x) = L_g(x) = 0$. On the other hand, $\Delta\Sigma(x)$ and $L_q(x)$ at the same scale are obtained as

$$\Delta\Sigma(x) = [\Delta u(x) + \Delta d(x)] + [\Delta \bar{u}(x) + \Delta \bar{d}(x)], \quad (24)$$

$$L_q(x) = q_L(x) + \bar{q}_L(x), \quad (25)$$

from the predictions of the CQSM shown in Fig.1. The logarithmically increasing behavior of $\Delta g(x, Q^2)$ and the logarithmically decreasing behavior of $L_g(x, Q^2)$ are just what has been pointed out in several previous papers [27],[34].

As pointed out in [27], $L_g(x, Q^2)$ at high energy scale is rather insensitive to the input distributions for orbital angular momentum at the starting energy, and it is basically determined by the polarized quark singlet and gluon distributions. On the other hand, the behavior of $L_q(x, Q^2)$ at the moderate value of Q^2 is strongly dependent on the input orbital angular momentum distribution. In fact, Fig.4 shows that $L_q(x, Q^2)$ remains positive at all the energy

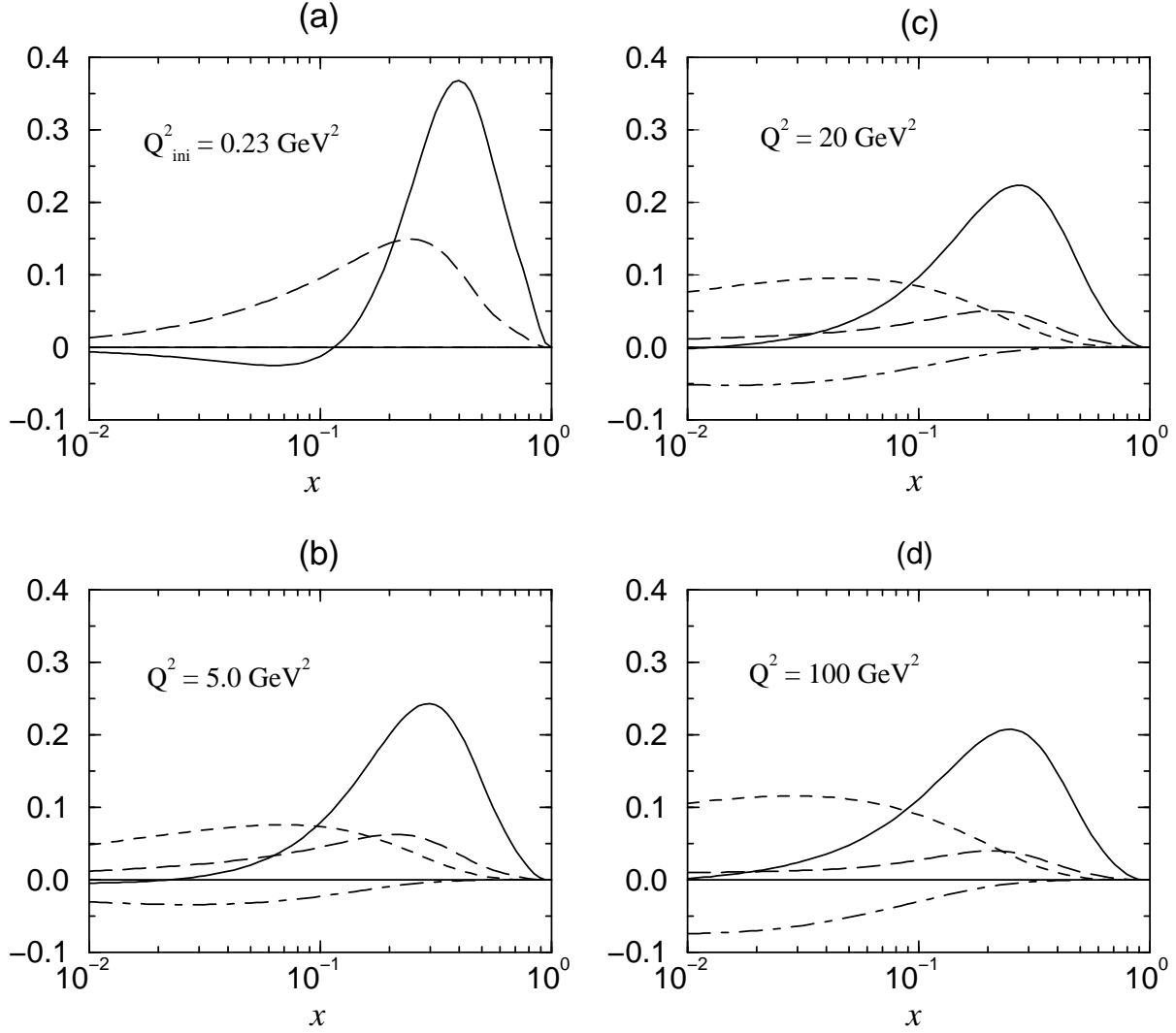


Figure 3: The LO evolutions of the spin and orbital angular momentum distribution functions for quarks and gluons. the solid and long-dashed curves respectively represent $x \Delta\Sigma(x, Q^2)$ and $x L_q(x, Q^2)$, whereas the dashed and dash-dotted curves stand for $x \Delta g(x, Q^2)$ and $x L_g(x, Q^2)$.

scales, although its magnitude gradually decreases as Q^2 increases. We point out that this behavior of $L_q(x, Q^2)$ is consistent with the scale dependence of the corresponding first moment $L_q(Q^2)$ shown in Fig.2(b).

Clearly, the origin of this unique behavior of $L_q(x, Q^2)$ and $L_q(Q^2)$ can be traced back to the extraordinary large and positive orbital angular momentum for quarks and antiquarks at the hadronic scale predicted by the CQSM. The results above may be compared with several previous investigations of the scale dependence of the orbital angular momentum distributions, the input distributions of which are prepared in a somewhat arbitrary way. For instance, two different scenarios have been investigated in [27]. The first scenario called the GRSV standard scenario has the property that $\frac{1}{2} \Delta\Sigma(Q_{ini}^2) + \Delta g(Q_{ini}^2) \simeq 0.475$ with very small orbital angular momentum for quarks and gluons, i.e. $L_q(Q_{ini}^2) + L_g(Q_{ini}^2) \simeq 0.015$. The second rather extreme scenario assumes very large gluon polarization such that $\Delta g(x, Q_{ini}^2) = g(x, Q_{ini}^2)$, which in turn dictates large and negative orbital angular momentum such that $L_q(Q_{ini}^2) + L_g(Q_{ini}^2) = -0.43$. A common feature of these scenarios is that the evolved $L_q(x, Q_{ini}^2)$ has large and negative values in wide range of x , which is quite different from the above-mentioned result of the CQSM shown in Fig.4. Unfortunately, any of these quite different scenarios cannot be excluded on the basis of our present knowledge, since all of these reproduces the available data for the longitudinally polarized deep-inelastic structure functions for the nucleon and the deuteron at least qualitatively. Highly desirable is some direct experimental information for any of $\Delta g(x, Q^2)$, $L_q(x, Q^2)$ and $L_g(x, Q^2)$.

4 Conclusions

An outstanding feature of the CQSM is that it can explain all the qualitatively noticeable features of the recent high-energy deep-inelastic-scattering observables including NMC data for $F_2^p(x) - F_2^n(x)$, $F_2^n(x)/F_2^p(x)$ [36], the Hermes [35] and NuSea [37] data for $\bar{d}(x) - \bar{u}(x)$, the EMC and SMC data for $g_1^p(x)$, $g_1^n(x)$ and $g_1^d(x)$ [21],[2], *without any free parameter* except for the starting energy scale of the DGLAP evolution equation [19],[20]. In the present paper, we have evaluated the spin and orbital angular momentum distribution functions within the same theoretical framework, and have investigated their scale dependences. It has been shown that the model can explain the smallness of the quark spin fraction at least qualitatively without assuming large gluon polarization at the low renormalization point. A key ingredient here is the large and positive orbital angular momentum carried by quarks and antiquarks with soft (small x) component. The predicted large and positive quark orbital angular momentum at

the low renormalization point necessarily affects the scenario of the scale dependence of the nucleon spin contents. The solution of the LO evolution equation indicates that the quark orbital angular momentum is a decreasing function of Q^2 and it may play insignificant role at the asymptotic energy scale, although the rate of reduction is quite slow beyond $Q^2 \simeq 5 \text{ GeV}^2$.

Acknowledgement

We would like to express our thanks to A. Schäfer and O. Martin for providing us with their evolution program for orbital angular momentum distributions and also for many helpful discussions. We are also grateful to V. Vento for clarifications on their results of Ref. [34].

References

- [1] EMC Collaboration, J. Ashman et al., Phys. Lett. **B206**, 364 (1988) ;
Nucl. Phys. **B328**, 1 (1989).
- [2] SMC Collaboration, B. Adeva et al., Phys. Rev. **D58**, 112001 (1998).
- [3] G. Altarelli and C.G. Ross, Phys. Lett. **B212**, 391 (1998) ;
R.D. Carlitz, J.C. Collins, and A.H. Muller, Phys. Lett. **B214**, 229 (1988) ;
A.V. Efremov and O.V. Teryaev, JINR Report E2-88-287 (1988).
- [4] T. Gehrmann and W.J. Stirling, Phys. Rev. **D53**, 6100 (1996) ;
R.D. Ball, S. Forte, and G. Ridolfi, Phys. Lett. **B378**, 255 (1996) ;
M. Glück, E. Reya, M. Stratmann, and W. Vogelsang, Phys. Rev. **D53**, 4775 (1996) ;
M. Stratmann, hep-ph/9910318.
- [5] S.J. Brodsky, J. Ellis, and M. Karliner, Phys. Lett. **B206**, 309 (1988).
- [6] M. Wakamatsu, Phys. Rev. **D42**, 2427 (1990).
- [7] M. Wakamatsu and H. Yoshiki, Nucl. Phys. **A524**, 561 (1991).
- [8] D.I. Diakonov and V.Yu. Petrov, Nucl. Phys. **B272**, 457 (1986).
- [9] D.I. Diakonov, V.Yu. Petrov, and P.V. Pobylitsa, Nucl. Phys. **B306**, 809 (1988).
- [10] For reviews, see, M. Wakamatsu, Prog. Theor. Phys. Suppl. **109**, 115 (1992) ;
Chr.V. Christov, A. Blotz, H.-C. Kim, P. Pobylitsa, T. Watabe, Th. Meissner,
E. Ruiz-Arriola, and K. Goeke, Prog. Part. Nucl. Phys. **37**, 91 (1996) ;
R. Alkofer, H. Reinhardt, and H. Weigel, Phys. Rep. **265**, 139 (1996).
- [11] E. Witten, in *Nuclear and Elementary Particle Physics*, eds. A. Chodos, E. Hadjimichael,
and C. Tze (World Scientific, Singapore, 1984).
- [12] T.H.R. Skyrme, Proc. Roy. Soc. (London) **A260**, 127 (1961).

- [13] G.S. Adkins, C.R. Nappi, and E. Witten, Nucl. Phys. **B228**, 552 (1983).
- [14] M. Wakamatsu, Prog. Theor. Phys. **95**, 143 (1996).
- [15] M. Wakamatsu and T. Watabe, Phys. Lett. **B312**, 184 (1993) ;
Chr.V. Christov, A. Blotz, K. Goeke, P. Pobylitsa, V.Yu. Petrov, M. Wakamatsu,
and T. Watabe, Phys. Lett. **B325**, 467 (1994).
- [16] M. Wakamatsu, Prog. Theor. Phys. **95**, 143 (1996).
- [17] D.I. Diakonov, M.V. Polyakov, and C. Weiss, Nucl. Phys. **B461**, 539 (1996).
- [18] B. Dressler, M. Maul, and C. Weiss, hep-ph/9906444.
- [19] M. Wakamatsu and T. Kubota, Phys. Rev. **D60**, 034020 (1999).
- [20] M. Wakamatsu and T. Watabe, hep-ph/9908425.
- [21] E143 Collaboration, K. Abe et al., Phys. Rev. **D58**, 112003 (1998) ;
E154 Collaboration, K. Abe et al., Phys. Rev. Lett. **79**, 26 (1997) ;
E155 Collaboration, P.L. Anthony et al., hep-ex/994002.
- [22] P. Hägler and A. Schäfer, Phys. Lett. **B430**, 179 (1998).
- [23] A. Harindranath and R. Kundu, Phys. Rev. **D59**, 116013 (1999).
- [24] P. Hoodbhoy, X. Ji, and W. Lu, Phys. Rev. **D59**, 074010 (1999).
- [25] R.L. Jaffe and A. Manohar, Nucl. Phys. **B536**, 303 (1990).
- [26] S.V. Bashinsky and R.L. Jaffe, Nucl. Phys. **B536**, 303 (1998).
- [27] O. Martin, P. Hägler, and A. Schäfer, Phys. Lett. **B448**, 99 (1999).
- [28] D.I. Diakonov, M.V. Polyakov, P.V. Pobylitsa, and C. Weiss, Phys. Rev. **D56**, 4069 (1997).
- [29] N. Mathur, S.J. Dong, K.F. Liu, L. Mankiewicz, and N.C. Mukhopadhyay, hep-ph/9912289.
- [30] S.J. Dong, J.-F. Lagaë, and K.F. Liu, Phys. Rev. Lett. **75**, 2096 (1995) ;
M. Fukugita, Y. Kuramashi, M. Okawa, and A. Ukawa, *ibid*, 2092 (1995).
- [31] X. Ji, J. Tang, and P. Hoodbhoy, Phys. Rev. Lett. **76** 740 (1996).
- [32] W. Furmanski and R. Petronzio, Z. Phys. **C11**, 293 (1982).
- [33] M. Glück, E. Reya, and A. Vogt, Z. Phys. **C48**, 471 (1990).
- [34] S. Scopetta and V. Vento, Phys. Lett. **B460**, 8 (1999).
- [35] HERMES Collaboration, K. Ackerstaff et al., Phys. Rev. Lett. **21**, 5519 (1998).
- [36] NMC Collaboration, P. Amaudruz et al., Phys. Rev. Lett. **66**, 2712 (1991).
- [37] E866 Collaboration, E.A. Hawker et al., Phys. Rev. Lett. **80**, 3715 (1998).